Available online at www.sciencedirect.com
SCIENCE DIRECT®
Journal of Luminescence 119–120 (2006) 258–263
JOURNAL OF LUMINESCENCE
www.elsevier.com/locate/jlumin

Upconversion luminescence properties of Y_2O_3:Yb^{3+}, Er^{3+} nanostructures

Gejihu De[b,c], Weiping Qin[a,b,*], Jishen Zhang[b], Jishuang Zhang[b,c], Yan Wang[b,c], Chunyan Cao[b,c], Yang Cui[b,c]

[a]*Institute of Electronic Science and Engineering, State Key Laboratory of Integrated Optoelectronics, Jilin University, Changchun 130012, China*
[b]*Changchun Institute of Optical, Fine Mechanics and Physics, Chinese Academy of Sciences, Key Laboratory of Excited State Processes, Chinese Academy of Sciences, Changchun 130033, China*
[c]*Graduate School of Chinese Academy of Sciences, Beijing 100039, China*

Available online 7 February 2006

Abstract

Cubic Y_2O_3 nanostructures doped with Yb^{3+} and Er^{3+} ions were synthesized by a facile hydrothermal method. Three distinct shapes such as nanotubes, nanospheres and nanoflakes formed in the products by adjusting the pH value of reacting solution. Powder X-ray diffraction analyses indicate that all the three nanostructures are pure cubic phase, while electron microscopy measurements confirm the formation of different morphologies. These nanostructures exhibit strong visible upconversion luminescence under the excitation of a 978-nm diode laser. In Yb^{3+}- and Er^{3+}-codoped Y_2O_3 nanocrystals, the relative intensity of green emission became stronger as the size and morphology of sample changed from tubes to flakes.

Keywords: Y_2O_3 nanostructures; Scanning and transmission electron microscopy; Luminescence; Size and morphology

1. Introduction

Nanostructure materials have attracted much attention in recent years because of their unique properties and potential applications in functional nanodevices [1]. It is generally accepted that these nanostructures provide an ideal system to investigate the dependence of electrical, optical, and mechanical properties on size and dimensionality. Rare earth (RE) compounds have been demonstrated in a wide range application such as high-performance magnets, luminescence materials and catalysts, and most of these functions depend strongly on the size and structure. Y_2O_3 doped with RE^{3+} phosphors is extensively used in optical display and light-emitting devices. The trend

*Corresponding author. 2699, Qianjin Street, Changchun 130012, China. Tel.: +86 431 6176352; fax: +86 431 4627031.
E-mail address: wpqin@public.cc.jl.cn (W. Qin).

0022-2313/$ - see front matter © 2006 Elsevier B.V. All rights reserved.
doi:10.1016/j.jlumin.2005.12.041

towards nanoscale science has raised interests in preparation of various Y_2O_3 nanostructures. In our previous report [2], Y_2O_3:Eu nanotubes were fabricated by surfactant self-assembly and their optical properties were investigated using laser selective spectroscopy. Recently, Yadong Li et al. reported the synthesis of RE nanotubes by a facile hydrothermal method, and their nanotubes have small inner diameters of 10 nm and single thin inorganic walls of about 1 nm [3,4]. Other type of Y_2O_3 structures such as nanoparticles and thin films have also been investigated extensively in order to develop highly efficient phosphors for light-emitting devices [5,6].

There is a growing interest in conversion of infrared radiation into shorter wavelengths by the materials doped with RE ions. Er^{3+} ion is an ideal candidate for this purpose due to its versatile energy levels in the near-infrared region. Codoping of Yb^{3+} ion as a sensitizer can yield a substantial improvement in upconversion efficiency due to the efficient energy transfer between the sensitizer and the emitter [7–9]. The availability of high-power infrared laser diodes has stimulated researchers to develop near-infrared to visible upconversion lasers, light-emitting devices and three-dimensional displays [10,11]. Furthermore, the upconverting phosphors have been used to enhance the near-infrared response of silicon solar cell [12]. This letter, reports the dependence of upconversion luminescence in Er^{3+}/Yb^{3+}-copoped Y_2O_3 nanostructures on morphology.

2. Experimental

The method for fabricating Y_2O_3:Yb^{3+}, Er^{3+} nanotubes is as follows: In a typical synthesis, 0.94 mmol Y_2O_3 (Aldrich), 0.04 mmol Yb_2O_3 (Aldrich) and 0.02 mmol Er_2O_3 (Aldrich) were dissolved in nitric acid (Aldrich 63%) to form clear aqueous solution, then 10% KOH solution was added to adjust the system to pH is about 6.0. The as-obtained colloidal precipitate was transferred into a 25 mL autoclave, sealed and kept at 160 °C for 3 day. After that, the autoclave was allowed to cool to room temperature naturally. The precipitate was then centrifuged, washed with deionized water to remove impurity ions in the final products, and dried at 200 °C in air. The resultant solid was put into a furnace. The furnace temperature was gradually raised to 500 °C (in air) and kept for 4 h. The synthesis of nanospheres and nanoflakes is similar to that of the nanotubes, but adjust the pH value of the reacting solution to be 6.5 and 7.0, respectively.

The crystal structures were analyzed by a Rigaku RU-200b X-ray powder diffractometer with CuKα radiation ($\lambda = 0.15406$ nm). The size and morphology were investigated by scanning transmission microscopy (SEM, KYKY 1000B) and transmission electron microscope (TEM, JEM 2010 with operating voltage of 200 kV). The upconversion luminescence spectra were recorded with a Hitachi F-4500 fluorescence spectrophotometer under the 978-nm excitation.

3. Results and discussion

The XRD patterns of the Y_2O_3:Yb^{3+}, Er^{3+} nanostructures are presented in Fig. 1, where (a), (b), and (c) curves correspond to nanotubes, nanospheres, and nanoflakes, respectively. The three samples exhibit identical patterns although they possess different morphologies. All the diffraction peaks can be readily indexed to a pure cubic phase [space group $Ia\bar{3}(2\,0\,6)$] with lattice

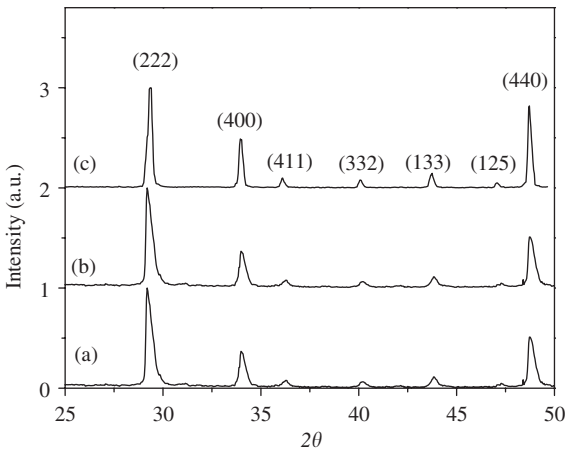

Fig. 1. XRD patterns of Y_2O_3:Yb,Er nanostructures: (a) nanotubes, (b) nanospheres, and (c) nanoflakes.

constant $a = 10.55$ nm, which are in good agreement with the standard values for the bulk cubic Y_2O_3 (JCPDS 74-1828).

Fig. 2(a) gives the TEM images of Y_2O_3:Yb^{3+}, Er^{3+} nanotubes. The central part of the cylindrical sample is white and the two peripheries are black, suggesting the formation of nanotubes. A bundle aggregate of nanotubes is also observed in the TEM image. The nanotubes appear to have a diameter of ~30 nm and a length up to several micrometers. The walls of nanotubes are estimated to be ~5 nm in thickness. The inset shows the electron diffraction pattern recorded perpendicularly to the nanotube long axis, which reveals that the nanotubes are single crystalline and also stable enough to withstand the irradiation of convergent high-energy electron beam. Fig. 2(b) and (c) show the SEM images of Y_2O_3:Yb^{3+}, Er^{3+} nanospheres and nanoflakes, respectively. The nanospheres are relatively uniform, with an average diameter of ~90 nm. Some cross sections of the nanoflakes can be observed in Fig. 2(c), from which the thickness of the nanoflakes is estimated to be ~50 nm. However, they are not uniform in lateral, varying from one half to 1μm.

Yb^{3+}-sensitized Er^{3+} ion is an efficient system for near-infrared to visible frequency upconversion. For Y_2O_3:Yb^{3+}, Er^{3+} nanostructures in this study, bright visible luminescence can be clearly observed with naked eyes under relatively weak 980-nm excitation, which promised the efficient upconversion nanophosphors. In Yb^{3+}/Er^{3+}-codoped materials, upconverted emission may result from different processes, including multistep excited state absorption (ESA), energy transfer (ET) between neighboring excited Er^{3+} ions, and APTE (Addition de photons par transfer d' Energie) between Yb^{3+} and Er^{3+} ions, among which APTE is the most efficient. Fig. 3 shows the energy levels and upconversion mechanism in Yb^{3+}/Er^{3+}-codoped system. A 978-nm photon excites an Yb^{3+} ion from the ground state $^2F_{7/2}$ to the excited state $^2F_{5/2}$, which may transfer the energy to a nearby Er^{3+} ion, promoting the Er^{3+}

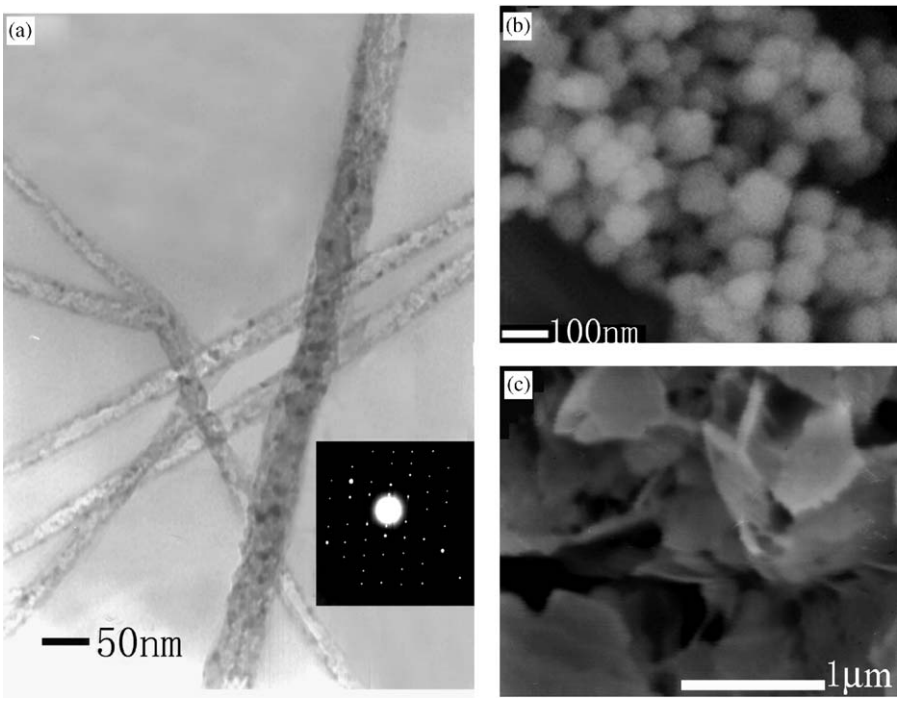

Fig. 2. (a) TEM image of Y_2O_3:Yb,Er nanotubes, the inset shows the electron diffraction pattern; (b) SEM image of Y_2O_3:Yb,Er nanospheres; and (c) SEM image of Y_2O_3:Yb,Er nanoflakes.

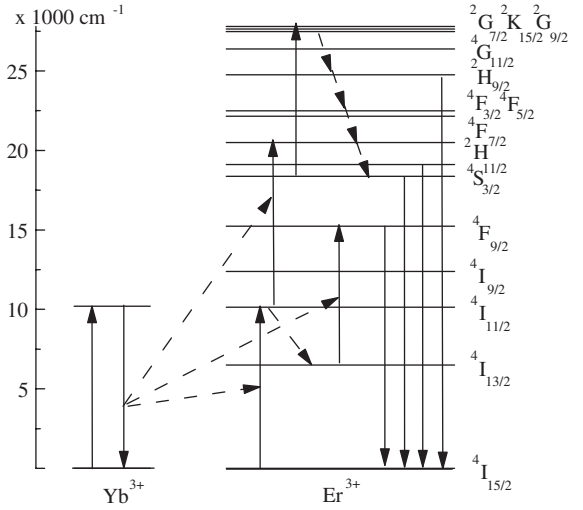

Fig. 3. Schematic diagram of Yb^{3+}- sensitized Er^{3+} upconversion luminescence under 978-nm excitation.

ion from $^4I_{15/2}$ to the $^4I_{11/2}$ state, and if the latter is already populated, the Er^{3+} ion may transit from the $^4I_{11/2}$ to the $^4F_{7/2}$ states. Subsequent nonradiative relaxations could populate the $^2H_{11/2}$ and $^4S_{3/2}$ states that are the emitting levels for the green luminescence. The $^4I_{11/2}$ states of Er^{3+} ions could be depopulated by an alternative relaxation route to $^4I_{13/2}$ states, which may be further excited to the red-emitting levels $^4F_{9/2}$, and the corresponding transition to the ground state $^4I_{15/2}$ produces red emission.

In Fig. 4(a), the red curve represents the room temperature upconversion emission spectrum of the Y_2O_3: Yb^{3+}, Er^{3+} nanotubes, where the red emission around 650 nm can be clearly observed and the green emission is very weak. The upconversion emission spectra of Y_2O_3:Yb^{3+}, Er^{3+} nanospheres and nanoflakes are illustrated by the green and blue curves, respectively. The spectra exhibit three distinct emission bands around 408, 520–570 and 650–670 nm, which correspond to the transitions $^2H_{9/2}\rightarrow{}^4I_{15/2}$ (blue emission), $^2H_{11/2}$, $^4S_{3/2}\rightarrow{}^4I_{15/2}$ (green emission), $^4F_{9/2}\rightarrow{}^4I_{15/2}$ (red emission), respectively. A significant feature of these spectra is that the relative intensity of upconversion emissions varies with the nanostructures of different morphologies. According to Fig. 4(a), while the integrated areas of peaks

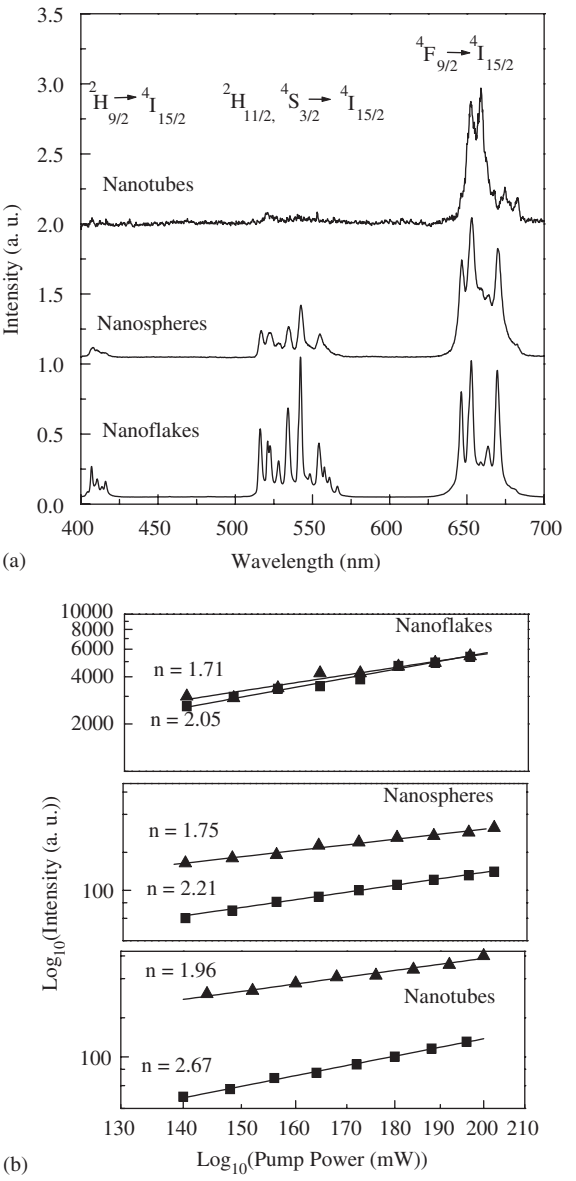

Fig. 4. (a) Room–temperature upconversion emission spectra of Y_2O_3:Yb, Er nanotubes, nanospheres, and nanoflakes, (b) Log–Log plot of upconversion intensity versus pump power in Y_2O_3:Yb,Er nanostructures. Uptriangles (▲) represent red emissions and squares (■) indicate green emissions.

are used to calculate the emission intensities. The intensity ratios of green emission to red emission are estimated to be 0.09, 0.33, and 0.87 for the nanotubes, nanospheres and nanoflakes, respectively. Such spectral change may result from

several factors such as host composition and doped concentration. However, in our case the three nanostructures were prepared through the similar hydrothermal method and the reaction systems were designed to have the same concentration of Yb^{3+} and Er^{3+} ions. Particularly, the pH value was adjusted very slowly under vigorous stirring so that the active ions were uniformly dispersed in the materials. Furthermore, XRD analysis has confirmed that all the three nanostructures possess cubic structure with the same lattice constant. Therefore, another effect, rather than the host composition and the doped concentration, should be considered to clarify the spectral differences among the three nanostructures.

Dependence of the upconversion luminescence intensity on pump power was performed to obtain a better understanding of the upconversion processes. For unsaturated upconversion luminescence, the emission intensity, I_{em}, is proportional to $I_{ex}{}^{n}$, where I_{ex} is the excitation intensity and the integer n is the order of upconversion process. More specifically, n is the number of pump photons required to populate the emitting state, which can be determined from the slope of Log–Log plot of upconversion intensity versus pump power. Fig. 4(b) shows the excitation dependence of the green (■) and red (▲) upconversion emissions for the Y_2O_3:Yb^{3+}, Er^{3+} nanostructures, where the fitting of the data yields straight lines and the values of the slopes are also listed. A gradual increase in the slope for both green and red emission can be seen while the material changes from large-sized nanoflakes to small-sized nanotubes. Particularly, the green emission of the nanotubes produces a slope value of 2.67, means that three-photon process may be partially involved in the green emission. According to Fig. 3, three-photon process generally populates the energy states ($^2G_{7/2}$, $^2K_{15/2}$, $^2G_{9/2}$). However, a fast cascade relaxation from these states to green-emitting levels may occur if there is a strong coupling between Er^{3+} ions and OH^- groups adsorbed on the nanotubes. Therefore, it is reasonable that the three-photon process practically leads to green emission in a typical material system with high-energy vibrations. On the other hand, the increase in the slope from nanoflakes to nanotubes further confirms that the presence of surface groups (OH^-) do have a great influence on the upconversion luminescence of the Y_2O_3:Yb^{3+}, Er^{3+} nanostructures.

When the material size approaches nanoscale, some energy states related to surfaces and interfaces appear to play an important role in determining the optical properties of RE-related luminescent materials [2]. Generally, such surface states are closely related to some anionic groups such as OH^- which originate from the precursors in the synthesis and cannot be removed even through a long time heat treatment. In our case, the nanostructures were prepared by the hydrothermal method. Its reasonable to conclude that certain amount of OH^- ions adsorbed on the surface exist. The OH^- group yields high-energy vibrational modes (3200–3600 cm^{-1}), compared to the intrinsic phonons of Y_2O_3 with a cutoff of phonon energy 597 cm^{-1}. These high-energy vibrations would strongly quench the excited states of Er^{3+} ions by multi-phonon relaxation, thus leading to a great influence on the upconversion processes. The multi-phonon relaxation rate, W_p, which can be expressed by the Miyakawa–Dexter equation [13],

$$W_p = W_p(0)\exp(-\alpha\Delta E/\hbar\omega), \tag{1}$$

$$\alpha = \ln\{p/g[n(t)+1]\} - 1, \tag{2}$$

$$p \approx \Delta E/\hbar\omega, \tag{3}$$

where g is the electron–phonon coupling strength, ΔE is the energy gap to the next lower level, $\hbar\omega$ is the phonon energy and the p is phonon numbers needed in the multi-phonon relaxation. For Er^{3+} ions, the $^4I_{11/2}$ and $^4I_{13/2}$ states are the intermediate levels responsible for green and red emissions, respectively. There is an energy gap of ~3600 cm^{-1} between the two states. According to Eq. (1), the high-energy vibrations from OH^- groups makes the multi-phonon relaxation ($^4I_{11/2} \rightarrow {}^4I_{13/2}$) much more probable than that of the intrinsic phonons in bulk Y_2O_3, where at least 6 phonons are required to bridge the gap. As is well known, the upconversion intensity depends on the population of the intermediate states. Therefore, the presence of OH^- groups on the surface would result in an

enhanced red emission and reduced green emission if they are coupled with Er^{3+} ions. To further clarify this effect, a relationship between upconversion emissions and Y_2O_3:Yb^{3+}, Er^{3+} nanostructures with different shapes was established. Here the ratio of surface area to volume is used to describe the three nanostructures since the materials with different dimensions and the size and morphology are correlated. With the surface to volume ratio increasing, there would be more and more Er^{3+} ions located near the surfaces, resulting in a stronger coupling between Er^{3+} and OH^-. Consequently, the green upconversion emission decreases compared to the red one, as the morphology changes from large-sized nanoflakes to small-sized nanotubes. Obviously, the presence of OH^- ions has similar quenching effect on the higher excited states that are responsible for the blue upconversion emissions.

4. Conclusion

Y_2O_3:Yb^{3+}, Er^{3+} nanostructures with different shapes, nanotubes, nanospheres and nanoflakes, were synthesized by adjusting the pH value of reacting solution in a hydrothermal method. The samples present strong visible upconversion luminescence with the excitation of a 978-nm diode laser. It is suggested that the OH^- groups adsorbed on the sample surface have a significant influence on the upconversion processes, leading to the variances in the relative intensity and pump–power dependence of the green and red emissions.

Acknowledgments

The authors would like to thank the support of the National Science Foundation of China (Grant no. 10274082 and no. 10474096).

References

[1] X. Peng, L. Manna, W. Yang, J. Wickham, E. Scher, A.P. Kadavanich, A. Alivisatos, Nature 404 (2000) 59.
[2] C. Wu, W. Qin, G. Qin, D. Zhao, J. Zhang, S. Huang, S. Lü, H. Liu, H. Lin, Appl. Phys. Lett. 82 (2003) 520.
[3] X. Wang, Y. Li, Angew. Chem. Int. Ed. 41 (2002) 4790.
[4] X. Wang, X. Sun, D. Yu, B. Zou, Y. Li, Adv. Mater. 15 (2003) 1442.
[5] G. Wakefield, E. Holland, P.J. Dobson, J.L. Hutchison, Adv. Mater. 13 (2001) 1557.
[6] D. Kumar, J. Sankar, K. Cho, G.V. Craciun, R.K. Singh, Appl. Phys. Lett. 77 (2002) 2518.
[7] G. Qin, W. Qin, S. Huang, C. Wu, D. Zhao, B. Chen, S. Lu, S. E. J. Appl. Phys. 92 (2002) 6936.
[8] G. Qin, W. Qin, C. Wu, S. Huang, J. Zhang, S. Lu, D. Zhao, H. Liu, J. Appl. Phys. 93 (2003) 4328.
[9] V. Fiorenzo, J.C. Boyer, J.A. Capobianco, S. Adolfo, M. Bettinelli, J. Phys. Chem. B. 107 (2003) 1107.
[10] D. Matsuura, Appl. Phys. Lett. 81 (2002) 4526.
[11] E. Downing, L. Hesselink, J. Ralston, R. Macfarlane, Science 273 (1996) 1185.
[12] A. Shalav, B.S. Richards, T. Trupke, K.W. Krämer, H.U. Güdel, Appl. Phys. Lett. 86 (1–3) (2005) 013505.
[13] T. Moyakawa, D.L. Dexter, Phys. Rev. B. 1 (1970) 2961.